

Micromechanical Approach to Strength properties of Steel Fiber Reinforced Concrete

Vanessa F. Pasa Dutra

Department of Civil Engineering
Federal University of Pelotas, Pelotas – RS, Brazil
vanessapasa@gmail.com

Samir Maghous

Department of Civil Engineering
Federal University of Rio Grande do Sul, Porto Alegre – RS, Brazil
samir.maghous@ufrgs.br

Américo Campos Filho

Department of Civil Engineering
Federal University of Rio Grande do Sul, Porto Alegre – RS, Brazil
americo@ufrgs.br

ABSTRACT

Combining the static approach of limit analysis and the periodic homogenization theory, the present paper is concerned with the assessment of the strength properties of steel fiber reinforced concrete (FRC). The macroscopic strength criterion for FRC can be theoretically obtained from the knowledge of the strength properties of the individual constituents, namely, concrete matrix and fibers. Adopting a Drucker-Prager failure condition for the concrete matrix and assuming a simplified geometrical model for fiber orientations and length, an approximate static-based model is formulated for the overall strength properties. Explicit analytical expressions have been derived emphasizing the reinforcing contribution of fiber addition. Additionally, numerical solutions are computed by means of finite element tool implementing an elastoplastic step-by-step algorithm. The main objective of the numerical approach is twofold: qualify the relevance of the analytical results and investigate the influence of real fiber morphology on the composite strength properties.

Keywords: Fiber Reinforced Concrete; Strength; Homogenization

1 INTRODUCTION

Evaluating the strength properties of materials remains fundamental concern in material and structural engineering, either for appropriate material use or for correct consideration in projects, design and verification stages. The strength capacities are classically characterized by the strength convex which defines the set of admissible stresses. Its determination is an important issue in material modeling.

As for most conventional materials, the concrete strength and behavior under multiaxial stress states have been experimentally and theoretically studied for several decades. These characteristics are mainly influenced by the physical and mechanical properties of aggregate and cement paste. In the case of fiber reinforced concrete (FRC), there are few experimental and analytical studies aimed

at establishing its behavior under complex stress states. Experimental studies performed by [1-5] sought to evaluate the steel FRC (SFRC) behavior under biaxial compression. These studies showed that the reinforced concrete has a failure curve distinct than the concrete matrix and the increase in the biaxial compression strength due to the fibers addition can reveal quite significant. In parallel to these experimental studies, the works of [6-8] were devoted to characterize the SFRC strength using empirical models, which allow estimating the strength of the concrete matrix reinforced by short fibers.

The limit analysis theory provides powerful tools for the assessment of the strength capacities of heterogeneous materials. Unlike elastoplastic analyses, application of limit analysis theorems leads to a straightforward approach to limit stress states of a structure since it does not involve a step by step analysis along the whole loading process. Limit analysis reasoning applied in the context of homogenization provides an appropriate framework for the formulation of macroscopic strength properties of a heterogeneous medium [9,10].

In this context, the purpose of this study is twofold. First, it formulates a simplified setting for analytical assessment of the homogenized strength properties of SFRC. Second, it presents finite element solutions obtained from elastoplastic step-by-step calculations that allow for assessing the accuracy of the simplified analytical predictions.

2 MACROSCOPIC STRENGTH DOMAIN

The aim of this section is to describe a simplified setting for fibers orientation and length that provides a periodic approximation of the SFRC microstructure. Then, combining the static approach of limit analysis and homogenization of periodic media, an approximate model for strength properties of SFRC is determined.

2.1 Matrix reinforced by long fibers in three direction

The determination of the macroscopic strength domain G^{hom} of a heterogeneous medium results from the resolution of a limit analysis problem defined on the representative elementary volume (REV) of the considered composite [9,10]. It requires solely the knowledge of the strength properties of the individual constituents (i.e., the matrix, fibers and fiber/matrix interface), together with the description of geometry, orientation and volume fraction of each constituent.

SFRC is a heterogeneous medium with random microstructure (Figure 1(a)) formed by a cementitious matrix and an isotropic distribution of short fibers. The strength properties of this kind of composite are expected to be isotropic. In what follows, f will refer to the volume fraction of fiber, l to the length of fiber and d to the diameter of fiber. The parameter l/d is the aspect ratio of fibers.

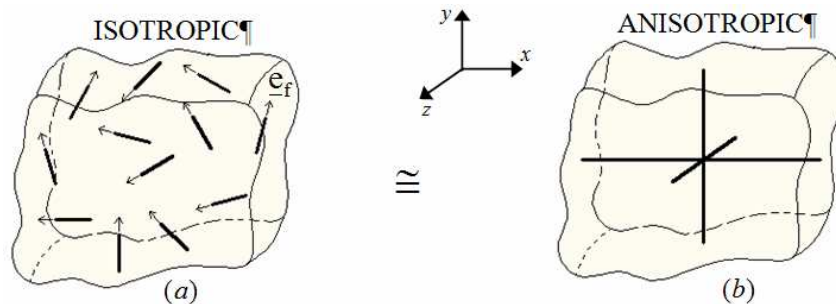


Figure 1: Representative elementary volume of SFRC and simplified periodic cell.

In the subsequent analysis, fundamental assumptions related to the geometry and orientation of fiber are introduced. More precisely, the approach is based on the heuristic consideration that the macroscopic strength domain of SFRC can be evaluated by approximating the microstructure of SFRC by means of a fictitious periodic medium. The latter is defined by the concrete matrix reinforced by a discrete distribution of long fibers arranged following p orientations of the space as sketched in Figure 1(b). Clearly enough, the higher is the number of fiber orientations p , the better is the estimate of G^{hom} . In particular, the obtained strength domain will tend to isotropy when increasing the value of p . However, in such a simplified model disregards *a priori* the effect of fiber aspect ratio on the strength properties of SFRC.

The calibration of the model, that is the correlation between the characteristics of the simplified geometrical model and those of SFRC, remains a crucial issue. In other words, what values of the strength parameters or volume fraction should be attributed to a given fiber set following the corresponding orientation. Mechanical properties of fiber reinforced composite, such as elastic or strength properties, are expected to depend on the aspect ratio of fibers and to tend toward asymptotic value as the aspect ratio increases [11]. The influence of the aspect ratio l/d on the composite strength properties can be evaluated from experimental data or numerical simulations. Since the effect of the aspect ratio is disregarded in the simplified approach, comparison of experimental or numerical results with the prediction of the analytical model developed in the sequel should theoretically provide guidelines for the calibration of the simplified model.

2.2 Macroscopic strength domain of a Matrix reinforced by long fibers

The situation depicted in Figure 1(b) refers to a periodic microstructure. The latter is completely described by the unit cell \mathcal{A} . The determination of the macroscopic strength domain G^{hom} of the periodic heterogeneous material reduces to solving a limit analysis problem defined on the aforementioned unit cell:

$$\underline{\underline{\Sigma}} \in G^{\text{hom}} \Leftrightarrow \exists \underline{\underline{\sigma}} \text{ such that } \begin{cases} \text{div } \underline{\underline{\sigma}} = 0, & \llbracket \underline{\underline{\sigma}} \rrbracket \cdot \underline{n} = 0, & \underline{\underline{\Sigma}} = \langle \underline{\underline{\sigma}} \rangle, & \underline{\underline{\sigma}} \cdot \underline{n} \text{ antiperiodic} \\ \underline{\underline{\sigma}}(\underline{x}) \in G^m \quad \forall \underline{x} \in \mathcal{A}^m, & \underline{\underline{\sigma}}(\underline{x}) \in G^f \quad \forall \underline{x} \in \mathcal{A}^f \quad f = 1, p \end{cases} \quad (1)$$

where $\underline{\underline{\Sigma}}$ and $\underline{\underline{\sigma}}$ represent respectively the macroscopic and microscopic stress fields. \mathcal{A}^m and \mathcal{A}^f are the geometric domains occupied respectively by the matrix and fiber $f \in \{1, \dots, p\}$. G^m (respectively, G^f) denotes the material strength domain at the current point $\underline{x} \in \mathcal{A}^m$ (respectively, \mathcal{A}^f). Tensor $\llbracket \underline{\underline{\sigma}} \rrbracket$ represents the jump of $\underline{\underline{\sigma}}$ when crossing any possible stress discontinuity surface with local normal \underline{n} . In this case (Eq. (1)), it is being considered perfect bonding at the fiber/matrix interface, which is equivalent to consider the material of the fiber/matrix interface with infinite strength.

A static estimate of convex G^{hom} can be derived by considering a piecewise homogeneous stress field complying with the required equilibrium and strength conditions, similarly to the approach proposed in de [12]. This stress distribution provides a lower bound estimate G_s^{hom} of G^{hom} , defined as

$$G_s^{\text{hom}} = \left\{ \begin{array}{l} \underline{\underline{\Sigma}} = \underline{\underline{\sigma}}^m + \sum_{f=1}^p f_f \sigma_f \underline{e}_f \otimes \underline{e}_f \\ \underline{\underline{\sigma}}^m \in G^m \quad \text{and} \quad \underline{\underline{\sigma}}^m + \sigma_f \underline{e}_f \otimes \underline{e}_f \in G^f \quad \forall f \in \{1, \dots, p\} \end{array} \right\} \subset G^{\text{hom}} \quad (2)$$

In the above equation, the unit vector \underline{e}_f defines the orientation of fiber number $f \in \{1, \dots, p\}$ and the parameter f_f is the volume fraction of the fiber oriented following \underline{e}_f , i.e., $f_f = |\mathcal{A}^f|/|\mathcal{A}|$. The quantity $f = \sum_{f=1}^p f_f$ represents the total reinforcement volume fraction.

In the particular situation of small reinforcement fraction, defined by $f_f \ll 1$, and the strength properties of fibers much higher than the matrix, i.e. $G^f \gg G^m$, [12] showed the following fundamental result:

$$G^{\text{hom}} \simeq G_s^{\text{hom}} = \left\{ \begin{array}{l} \underline{\underline{\Sigma}} = \underline{\underline{\sigma}}^m + \sum_{f=1}^p \sigma_f \underline{e}_f \otimes \underline{e}_f \\ \underline{\underline{\sigma}}^m \in G^m, \quad \sigma_f \in [\tilde{\sigma}_f^-, \tilde{\sigma}_f^+] \end{array} \right\} \quad (3)$$

where $\tilde{\sigma}_f^+ = f_f \sigma_f^+$ and $\tilde{\sigma}_f^- = f_f \sigma_f^-$ represent respectively the fiber uniaxial tensile and compressive strengths per unit transverse area. Parameters σ_f^+ and σ_f^- are respectively the tensile and compressive strengths of fiber constitutive material.

In what follows, we shall restrict the study to the particular situation in which the SFRC is modeled by means of concrete matrix reinforced by a tri-directional array ($p=3$) of mutually orthogonal fibers, oriented following the axes of a reference frame $Oxyz$. It is emphasized that the approximation $G^{\text{hom}} \simeq G_s^{\text{hom}}$ given in Eq. (3) holds for the case of SFRC. Indeed, the amount of steel fibers is in practice very small ($f < 5\%$), and the strength of steel can be considered as sufficiently higher than that of concrete.

Geometrically, the strength domain G^{hom} for the composite reinforced by a tri-directional array of mutually perpendicular fibers can be interpreted in the space $\mathbb{R}^6 = \{\Sigma_{xx}, \Sigma_{yy}, \Sigma_{zz}, \Sigma_{xy}, \Sigma_{xz}, \Sigma_{yz}\}$ of macroscopic stresses as the convex envelope of eight domains obtained by translating the matrix strength domain by algebraic distances $f_x \sigma_x^-$ and $f_x \sigma_x^+$ along the Σ_{xx} -axis, $f_y \sigma_y^-$ and $f_y \sigma_y^+$ along the Σ_{yy} -axis and $f_z \sigma_z^-$ and $f_z \sigma_z^+$ along the Σ_{zz} -axis [13]. These translations in the space of macroscopic stresses are the expression of the reinforcement due to the presence of fibers. Thereby, one can identify zones along the boundary of G^{hom} where one, two or three of the stress parameters σ_f , $f \in \{x, y, z\}$, has one or other of its limit values. Zones identified as A are those in which only one stress parameter (σ_x , σ_y or σ_z) has a limit value whilst zones B and C are those in which two and three parameters, respectively, have a limit value.

The strength domains G^m and G^{hom} of the matrix and composite can be conveniently defined by means of associated strength criterion F^m and F^{hom} , respectively:

$$F^{\text{hom}}(\underline{\underline{\Sigma}}) \leq 0 \Leftrightarrow \begin{cases} \underline{\underline{\Sigma}} = \underline{\underline{\sigma}}^m + \sum_{i=1}^3 \sigma_f \underline{e}_f \otimes \underline{e}_f \\ F^m(\underline{\underline{\sigma}}^m) \leq 0, \quad \sigma_f \in I_f \quad f = x, y, z \end{cases} \quad (4)$$

with $I_f = [\tilde{\sigma}_f^-, \tilde{\sigma}_f^+]$, recalling that $\tilde{\sigma}_f^\pm = f_f \sigma_f^\pm$.

From a mathematical viewpoint, the expression of $F^{\text{hom}}(\underline{\underline{\Sigma}})$ is obtained by the following minimization process with respect to constrained parameters σ_x , σ_y and σ_z

$$F^{\text{hom}}(\underline{\underline{\Sigma}}) = \min_{\sigma_f \in I_f \quad f=x,y,z} F^m(\underline{\underline{\Sigma}} - \sigma_x \underline{e}_x \otimes \underline{e}_x - \sigma_y \underline{e}_y \otimes \underline{e}_y - \sigma_z \underline{e}_z \otimes \underline{e}_z) \quad (5)$$

Denoting by $\overset{\circ}{I}_f =]\tilde{\sigma}_f^-, \tilde{\sigma}_f^+[$ and $\partial I_f = \{\tilde{\sigma}_f^-, \tilde{\sigma}_f^+\}$, the following situations can be identified:

- The situation defined by $\sigma_f \in \partial I_f$ for the three fiber stress parameters. In this situation, the expression of $F^{\text{hom}}(\underline{\underline{\Sigma}})$ is given by

$$F^{\text{hom}}(\underline{\underline{\Sigma}}) = F^m(\underline{\underline{\Sigma}} - \sigma_x \underline{e}_x \otimes \underline{e}_x - \sigma_y \underline{e}_y \otimes \underline{e}_y - \sigma_z \underline{e}_z \otimes \underline{e}_z) \quad (6)$$

since the values of all stress parameters are fixed: $\sigma_x = \tilde{\sigma}_x^\pm$, $\sigma_y = \tilde{\sigma}_y^\pm$ and $\sigma_z = \tilde{\sigma}_z^\pm$. This situation refers to zones C along the boundary of G^{hom} .

- The situations when two of the three stress parameters have a limit value: $(\sigma_x \in \partial I_x, \sigma_y \in \partial I_y, \sigma_z \in \overset{\circ}{I}_z)$ and circular permutations of x , y and z . Since, for instance, σ_x is fixed to $\tilde{\sigma}_x^+$ or $\tilde{\sigma}_x^-$ and σ_y to $\tilde{\sigma}_y^+$ or $\tilde{\sigma}_y^-$, $F^{\text{hom}}(\underline{\underline{\Sigma}})$ results from solving:

$$\frac{\partial F^m}{\partial \sigma_{zz}}(\underline{\underline{\Sigma}} - \sigma_x \underline{e}_x \otimes \underline{e}_x - \sigma_y \underline{e}_y \otimes \underline{e}_y - \sigma_z \underline{e}_z \otimes \underline{e}_z) = 0 \quad (7)$$

with respect to σ_z . This situation refers to zones B along the boundary of G^{hom} .

- The situations when only one of the stress parameters has a limit value: $(\sigma_x \in \partial I_x, \sigma_y \in \overset{\circ}{I}_y, \sigma_z \in \overset{\circ}{I}_z)$ and circular permutations of x , y and z . The expression of $F^{\text{hom}}(\underline{\underline{\Sigma}})$ is obtained by solving:

$$\frac{\partial F^m}{\partial \sigma_{ii}}(\underline{\underline{\Sigma}} - \sigma_x \underline{e}_x \otimes \underline{e}_x - \sigma_y \underline{e}_y \otimes \underline{e}_y - \sigma_z \underline{e}_z \otimes \underline{e}_z) = 0, \quad \text{with } i = y, z \quad (8)$$

with respect to σ_y and σ_z , the parameter σ_x being fixed to $\tilde{\sigma}_x^+$ or $\tilde{\sigma}_x^-$. The complementary cases are obtained by circular permutation. This situation refers to zones A along the boundary of G^{hom} .

- The last situation is defined by $(\sigma_x \in \overset{\circ}{I}_x, \sigma_y \in \overset{\circ}{I}_y, \sigma_z \in \overset{\circ}{I}_z)$. The strength criterion is obtained by solving, with respect to parameters σ_x , σ_y and σ_z , the following system:

$$\frac{\partial F^m}{\partial \sigma_{ii}} (\underline{\underline{\Sigma}} - \sigma_x \underline{e}_x \otimes \underline{e}_x - \sigma_y \underline{e}_y \otimes \underline{e}_y - \sigma_z \underline{e}_z \otimes \underline{e}_z) = 0, \text{ with } i = x, y, z \quad (9)$$

2.3 The case of a Drucker-Prager matrix

The strength capacities of the concrete matrix are assumed to be described by a Drucker-Prager. The Drucker-Prager criterion may be expressed in the following form:

$$F^m(\underline{\underline{\sigma}}) = \sqrt{\frac{3}{2}} \|\underline{\underline{s}}\| + \alpha_m (\text{tr} \underline{\underline{\sigma}} - \sigma_m) - \sigma_m \leq 0 \quad (10)$$

where $\|\underline{\underline{s}}\| = (\underline{\underline{s}} : \underline{\underline{s}})^{1/2}$ is the norm of the deviatoric stress tensor $\underline{\underline{s}} = \text{dev}(\underline{\underline{\sigma}})$. The material parameter σ_m represents the uniaxial tensile strength. Scalar α_m is a non-dimensional parameter ranging between 0 and 1, which accounts for the criterion dependence on the hydrostatic stress.

Observing that $\frac{\partial F^m}{\partial \underline{\underline{\sigma}}} = \sqrt{\frac{3}{2}} \underline{\underline{s}} / \|\underline{\underline{s}}\| + \alpha_m \underline{\underline{1}}$, Eq. (7) corresponding to the boundary B of G^{hom} leads to the following minimizing parameter that defines the fiber stress parameter σ_z :

$$\sigma_z^0 = \frac{3}{2} \left(S_{zz} + \frac{(\sigma_x + \sigma_y)}{3} + \sqrt{\frac{2}{3}} \frac{\alpha_m}{\sqrt{1 - \alpha_m^2}} \sqrt{\underline{\underline{S}} : \underline{\underline{S}} - \frac{3}{2} S_{zz}^2 + \frac{(\sigma_x - \sigma_y)^2}{2} - (\sigma_x - \sigma_y)(S_{xx} - S_{yy})} \right) \quad (11)$$

where $\underline{\underline{S}} = \text{dev}(\underline{\underline{\Sigma}})$ is the deviatoric part of the macroscopic stress tensor. Taking into account the restriction $\sigma_z \in \overset{\circ}{I}_z$, this parameters is thus given by

$$\sigma_z(\underline{\underline{\Sigma}}) = \begin{cases} f_z \sigma_z^- & \text{if } \sigma_z^0 \leq f_z \sigma_z^- \\ \sigma_z^0 & \text{with } \sigma_x = f_x \sigma_x^+ \text{ and } \sigma_y = f_y \sigma_y^- \\ & \text{or } \sigma_x = f_x \sigma_x^- \text{ and } \sigma_y = f_y \sigma_y^+ \quad \text{if } \sigma_z^0 \in \overset{\circ}{I}_z \\ f_z \sigma_z^+ & \text{if } \sigma_z^0 \geq f_z \sigma_z^+ \end{cases} \quad (12)$$

The remaining zones B are obtained by proceeding to circular permutations of x, y and z in the above Eq. (11) and (12).

As regards the zones A of the boundary of G^{hom} , the system of Eq. (8) yields:

$$\begin{cases} \sigma_y^0 = 2S_{yy} + S_{zz} + \sigma_x + 2\sqrt{3} \frac{\alpha_m}{\sqrt{1-4\alpha_m^2}} \sqrt{S_{xy}^2 + S_{xz}^2 + S_{yz}^2} \\ \sigma_z^0 = 2S_{zz} + S_{yy} + \sigma_x + 2\sqrt{3} \frac{\alpha_m}{\sqrt{1-4\alpha_m^2}} \sqrt{S_{xy}^2 + S_{xz}^2 + S_{yz}^2} \end{cases} \quad (13)$$

σ_x being fixed to $\tilde{\sigma}_x^+$ or $\tilde{\sigma}_x^-$. Restrictions $\sigma_y \in I_y$ and $\sigma_z \in I_z$ impose thus

$$\sigma_y(\underline{\Sigma}) = \begin{cases} f_y \sigma_y^- & \text{if } \sigma_y^0 \leq f_y \sigma_y^- \\ \sigma_y^0 & \text{with } \sigma_x = f_x \sigma_x^+ \text{ if } \sigma_y^0 \in I_y \\ f_y \sigma_y^+ & \text{if } \sigma_y^0 \geq f_y \sigma_y^+ \end{cases} \quad \text{and} \quad \sigma_z(\underline{\Sigma}) = \begin{cases} f_z \sigma_z^- & \text{if } \sigma_z^0 \leq f_z \sigma_z^- \\ \sigma_z^0 & \text{with } \sigma_x = f_x \sigma_x^+ \text{ if } \sigma_z^0 \in I_z \\ f_z \sigma_z^+ & \text{if } \sigma_z^0 \geq f_z \sigma_z^+ \end{cases} \quad (14)$$

The remaining zones A are obtained by circular permutations of x, y and z in the above equations (13 and 14).

The last situation is that where all stress parameters σ_f , $f \in \{x, y, z\}$ have no limit value. In this case, the stress parameters σ_f , $f \in \{x, y, z\}$ solutions to system (9) are obtained after some mathematical developments

$$\sigma_f^0 = \Sigma_{ff} - \frac{1+\alpha_m}{3\alpha_m} \sigma_m \quad f = x, y, z \quad (15)$$

The corresponding regions of convex G^{hom} are obtained by taking the projection of each one of the stress parameters σ_f^0 onto interval I_f : $\sigma_f = \text{Pr oj}_{I_f}(\sigma_f^0)$. This situation can occur only for macroscopic stress states such that $\Sigma_{xy} = \Sigma_{xz} = \Sigma_{yz} = 0$. The strength conditions reduces that to

$$\tilde{\sigma}_f^- + \frac{1+\alpha_m}{3\alpha_m} \sigma_m \leq \Sigma_{ff} \leq \tilde{\sigma}_f^+ + \frac{1+\alpha_m}{3\alpha_m} \sigma_m \quad f = x, y, z \quad (16)$$

3 FINITE ELEMENT NUMERICAL SIMULATIONS

In the simplified setting defined in section 2, an analytical estimate of the strength capacities of SFRC has been derived. The latter is based on the fundamental approximation that the reinforcing effects of fibers can be evaluated by considering three orthogonal families for fiber orientation. This is clearly a strong simplification since in SFRC the fiber distribution is rather isotropic. In order to evaluate the relevancy and accuracy of such approximation on the effective strength properties of SFRC, finite element simulations are performed on a REV of cement matrix reinforced by randomly distributed short fibers. The macroscopic limit stress states are evaluated by means of step-by-step elastoplastic analysis until the free plastic flow of the structure is reached.

A cubic REV Ω of side $2l_{\text{VER}}$ is considered (Figure 2). Symmetry with respect to mid-planes $x=0$, $y=0$ and $z=0$, is assumed for the spatial distribution of fibers. A biaxial macroscopic

stress solicitation $\underline{\underline{\Sigma}} = \Sigma_I \underline{e}_x \otimes \underline{e}_x + \Sigma_{II} \underline{e}_y \otimes \underline{e}_y$ is simulated by imposing the following mixed conditions on the boundary of the REV: (a) stress-free conditions on the horizontal faces $z = \pm l_{VER}$ and (b) frictionless interface conditions on the vertical sides, along which the normal displacement $\xi_x = \pm E_0 l_{VER}$ along sides $x = \pm l$ and $\xi_y = \pm \gamma E_0 l_{VER}$ along sides $y = \pm l$ are imposed. $E_0 < 0$ is a fixed strain parameter and γ is a non-dimensional parameter that allows investigating different loading paths in the plane (Σ_I, Σ_{II}) . Perfect bonding is assumed between the concrete matrix and fibers.

Owing to the symmetry conditions, only an eighth of the REV geometry, with appropriate boundary conditions, is considered for the numerical analysis (Figure 2).

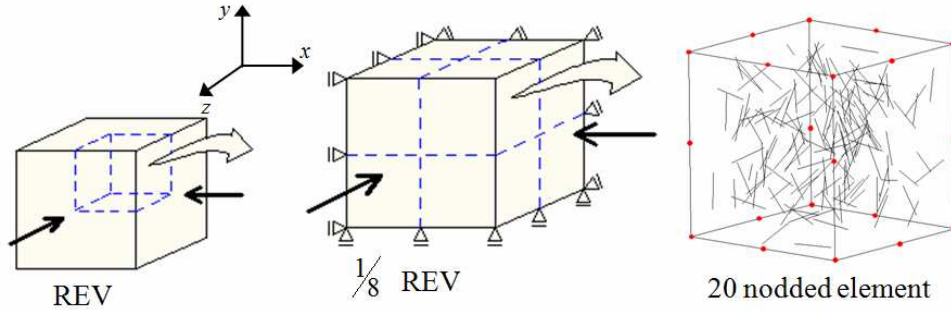


Figure 2: REV and macroscopic strain considered for the FE simulations.

Twenty noded quadratic hexahedral elements were used for the discretization of the concrete matrix geometry. As regards the reinforcement components, the fibers were randomly generated and embedded within the concrete matrix finite elements. We herein refer to the so-called “embedded model” [14], commonly used in the analysis of reinforced concrete structures. In this model the fibers location and geometry are independent of the finite element mesh. The displacements of the fibers are related to the displacements of the matrix finite element nodes where they are located and it is considered that each fiber has the same kinematics than the coincident points of the embedding concrete matrix finite element.

The reinforcement elements thus considered contribute to the rigidity and the internal work of the element (or elements) in which they are embedded. In the context of the “embedded model” formulation, the stiffness matrix and internal force vector related to the fibers are added, respectively, to the stiffness matrix and the of internal nodal forces vector of the corresponding matrix element. The spatial distribution and orientation of fibers were randomly generated by means of a specific procedure using the intrinsic function RAN of Fortran programming language.

Elastic-perfectly plastic behaviors with associated plastic flow rules were adopted for both constituent of SFRC. The yield function of concrete matrix is described by the Drucker Prager criterion Eq. (10), while the steel bars are assumed to take only uniaxial tensile-compressive stresses subject to a yield condition of the type $\sigma_f^- \leq \sigma \leq \sigma_f^+$. The iterative algorithm used for plastic integration (return mapping) is described in most handbooks of computational plasticity. The macroscopic stress is computed as

$$\underline{\underline{\Sigma}} = \langle \underline{\underline{\sigma}} \rangle = \frac{1}{|\Omega|} \int_{\Omega} \underline{\underline{\sigma}}(\underline{x}) \, d\Omega = \int_{\partial\Omega} \underline{x} \otimes (\underline{\underline{\sigma}} \cdot \underline{n}) \, dS \quad (17)$$

The following values for the REV side and fiber length were adopted in the numerical simulations: $l_{VER} = 20 \text{ cm}$ and $l = 3 \text{ cm}$, respectively. Two values were considered for the fiber aspect ratio: $l/d = 20$ and 100 , and three values for the volume fraction of fibers have been used: $f = 0.5 \%$, $f = 2 \%$ and $f = 5 \%$.

The strength surface parameters σ_m and α_m were identified by fitting the concrete uniaxial and biaxial compressive strengths. Only compressive stresses have been investigated. Two concrete matrices have been studied. They correspond to distinct uniaxial compressive strengths, $f_c^m = 30 \text{ MPa}$ and 70 MPa , and biaxial compressive strengths equal to $f_{cb}^m = 1,16 f_c^m$. For the steel fibers, values of $\sigma_f^+ = -\sigma_f^- = 1000 \text{ MPa}$ were adopted.

A strain parameters $E_0 = -0.05$ was incrementally applied, with parameter γ ranging between -0.5 and 1 . Each value of the loading path parameter γ is associated with a limit stress state (Σ_I, Σ_{II}) .

For comparison purposes, the predictions from the analytical approximation described in the previous section are evaluated assuming an equivalent fiber distribution along the three orthogonal directions $(\underline{e}_x, \underline{e}_y, \underline{e}_z)$. In other terms, it was assumed that $f_x = f_y = f_z = f/3$ and $\sigma_x^\pm = \sigma_y^\pm = \sigma_z^\pm = \sigma_f^\pm$. It is important to note that we examined the situation where the principal macroscopic stresses are oriented following the directions $(\underline{e}_x, \underline{e}_y, \underline{e}_z)$ of fibers.

Figure 3 shows FE results together with the corresponding analytical predictions. The solid lines represent the analytical predictions obtained for the strength domain of steel FRC, while the symbols refer to the numerical results.

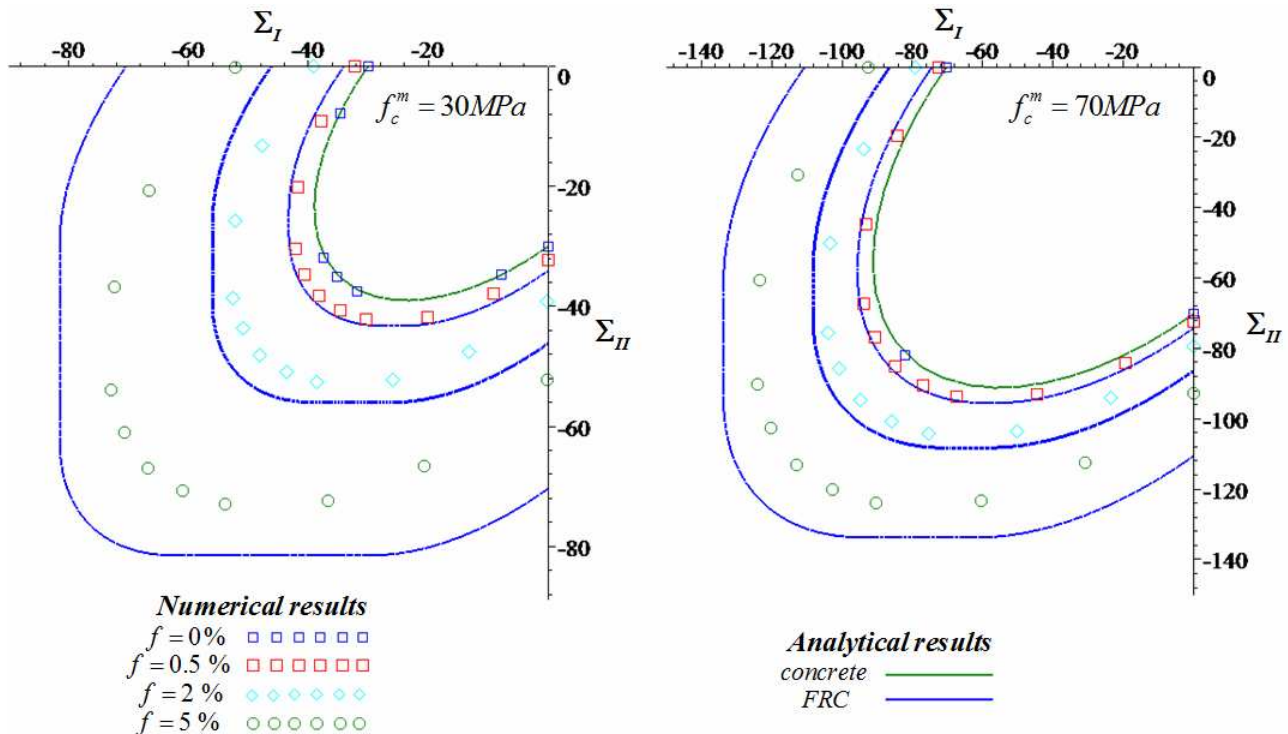


Figure 3: Strength domain of SFRC for biaxial stresses: numerical results versus analytical predictions.

It is first emphasized that numerical simulations with fiber aspect ratios $l/d = 20$ and $l/d = 100$ have led to very close results. This preliminary results suggest that the aspect ratio of fiber has a negligible influence on the strength properties of usual SFRC ($f \leq 5\%$ and $l/d = 20 - 100$). In particular, the assumption of long fibers adopted for the analytical model seems reasonable for the assessment of SFRC strength properties, similarly to what has been obtained in [15] for the elastic properties of SFRC.

The comparison of the two approaches indicates that the analytical predictions overestimate the strength of the medium reinforced by randomly distributed short fibers, particularly under uniaxial compressive stress. Since the aspect ratio is not affecting significantly the strength properties of SFRC, this is clearly attributed to the fact that large amount of fibers (third of total fiber content) is concentrated along the directions \underline{e}_x and \underline{e}_y of macroscopic solicitation. Since fibers are isotropically distributed in SFRC, the simplified model that is concentrating the fiber distribution along the principal directions of loading is naturally expected to overestimate the strength properties of SFRC. A modeling including a higher number of fiber directions would undoubtedly improve the predictions of SFRC strength properties.

4 IMPROVEMENT OF BIAXIAL AND UNIAXIAL COMPRESSIVE STRENGTH ESTIMATES

The finite element analysis showed that the analytical model based on three fixed orientations of fibers leads to predictions that are higher than the numerical solutions obtained from reasoning on a REV of SFRC. The aim of this section is to develop an improved approach to biaxial and uniaxial compressive strengths of SFRC. The idea of the approach may be summarized as follows. The tridirectional fiber reinforced composite is kept as a simplified model for representing the morphology of SFRC. The approach consists basically in two steps. In the first step, the limit state of a macroscopic stress, defined by the orientation of its principal directions with respect to fibers, is evaluated. The second step consists in averaging the obtained limit stress over all orientations of the space, leading thus to an isotropic estimate. In some extent, this approach that can be applied to any stress loading, consists in fact to an isotropization process of the strength properties. In the subsequent analysis, we consider the specific cases of compressive biaxial and uniaxial macroscopic stress loading.

4.1 Biaxial compressive strength

The biaxial compressive solicitation of the REV is defined as $\underline{\underline{\Sigma}} = \Sigma (\underline{e}_I \otimes \underline{e}_I + \underline{e}_{II} \otimes \underline{e}_{II})$, with $\Sigma < 0$. The unit vectors \underline{e}_I and \underline{e}_{II} refers to the orientation of stress principal directions. The latter is completely defined by means of three angles (θ, ϕ, ψ) (Euler angles) with respect to the fixed frame $(\underline{e}_x, \underline{e}_y, \underline{e}_z)$ of fibers (Figure 4).

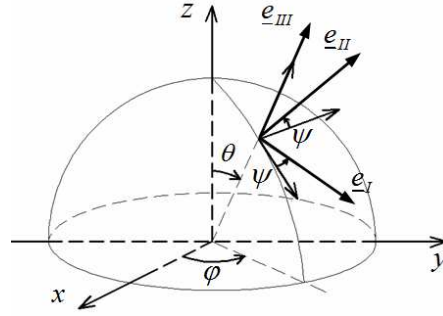


Figure 4: Euler angles defining the orientation of principal stress directions, and fibers directions $(\underline{e}_x, \underline{e}_y, \underline{e}_z)$.

The first step is to evaluate the strength under biaxial compressive stress $\Sigma_b^-(\theta, \varphi, \psi)$. The latter is obtained through the minimization procedure defined in Eq. (5). Applying the latter to the considered solicitation yields:

$$\Sigma_b^-(\theta, \varphi, \psi) = \min \left\{ \Sigma \mid \underline{\underline{\Sigma}} = \Sigma(\underline{e}_I \otimes \underline{e}_I + \underline{e}_{II} \otimes \underline{e}_{II}); \underline{\underline{\sigma}}^m = \underline{\underline{\Sigma}} - \sum_{i=1}^3 \sigma_f \underline{e}_f \otimes \underline{e}_f; \right. \quad (18)$$

$$\left. F^m(\underline{\underline{\sigma}}^m) \leq 0; |\sigma_f| \leq f_f \sigma_f^+, f = x, y, z \right\}$$

Basic developments of Eq. (18) lead to the following expression

$$\Sigma_b^-(\theta, \varphi, \psi) = \min \left\{ \frac{-\sum_{f=1}^3 \sigma_f (2(1+2\alpha_m^2) - 3(a_{1f}^2 + a_{2f}^2)) - 4\alpha_m(\alpha_m + 1)\sigma_m - \sqrt{\beta}}{2(1-4\alpha_m^2)}, |\sigma_f| \leq f_f \sigma_f^+, f = x, y, z \right\} \quad (19)$$

$$\beta = \left(\sum_{f=1}^3 \sigma_f (2(1+2\alpha_m^2) - 3(a_{1f}^2 + a_{2f}^2)) + 4\alpha_m(\alpha_m + 1)\sigma_m \right)^2$$

$$- 4(1-4\alpha_m^2) \left(- \left(\sigma_m + \sum_{f=1}^3 \sigma_f \alpha_m + \sigma_m \right)^2 + \sum_{f=1}^3 \sigma_f^2 - \sigma_x \sigma_y - \sigma_y \sigma_z - \sigma_z \sigma_x \right)$$

Coefficients a_{ij} define the components of vectors \underline{e}_I , \underline{e}_{II} and \underline{e}_{III} in the fixed frame $(\underline{e}_x, \underline{e}_y, \underline{e}_z)$. The analytical expression of $\Sigma_b^-(\theta, \varphi, \psi)$ determined from Eq. (19) requires some complex developments that involve a discussion with respect of the stress orientation (θ, φ, ψ) . Instead, $\Sigma_b^-(\theta, \varphi, \psi)$ is computed by means of numerical minimization.

The second step of the approach consists in adopting for the biaxial compressive strength the following average value

$$f_{cb} = \langle \Sigma_b^- \rangle = \frac{1}{4\pi^3} \int_0^{2\pi} \int_0^\pi \int_0^{2\pi} \Sigma_b^-(\theta, \varphi, \psi) d\psi d\theta d\varphi \quad (20)$$

The obtained estimate is compared to the results derived from finite element simulations. Two different concrete matrices, corresponding to uniaxial compressive strengths f_c^m equals to 30 MPa and 70 MPa, are considered.

The semi-analytical estimate of the biaxial compressive strength $f_{cb} = \langle \Sigma_b^- \rangle$ defined in Eq. (20) is also compared to experimental data available in [3] and [5]. In their laboratory tests, [3] employed fibers with aspect ratio $l/d = 70$ and three volume fraction of fibers $f = 0.5\%$, $f = 1\%$ and $f = 1.5\%$. The uniaxial and the biaxial compressive strength of tested concrete were respectively, $f_c^m = 82.3 \text{ MPa}$ and $f_{cb}^m = 1.20 f_c^m$. The values of parameters defining the Drucker-Prager criterion were identified accordingly: $\alpha_m = 0.141$ and $\sigma_m = 61.93 \text{ MPa}$. The uniaxial tensile strength of used fibers was 1115 MPa. [5] employed fibers with aspect ratio $l/d = 44$ and three volume fraction of fibers $f = 0.5\%$, $f = 1\%$. The uniaxial and the biaxial compressive strength of the concrete matrix tested by this author were, respectively, $f_c^m = 28.24 \text{ MPa}$ and $f_{cb}^m = 1.16 f_c^m$. The values for the parameters of the Drucker-Prager criterion to be introduced in the model have been identified $\alpha_m = 0.121$ and $\sigma_m = 23.13 \text{ MPa}$. The uniaxial tensile strength of the fibers was 1200 MPa.

Figure 5(a) shows the variations of the estimate of biaxial compressive strength as a function of the volume fraction of steel fibers for usual values of f ranging between 0.5% and 5%. Figure 5(b) shows the semi-analytical estimates of $f_{cb} = \langle \Sigma_b^- \rangle$ together with the experimental results of [3] and [5].

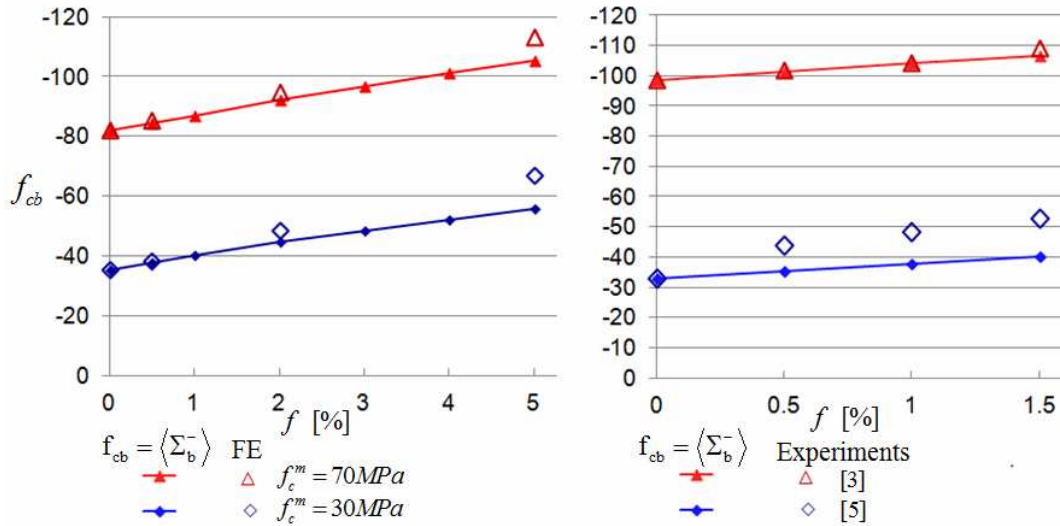


Figure 5: Improved estimates of biaxial compressive strength $f_{cb} = \langle \Sigma_b^- \rangle$ versus fiber volume fraction.

Comparison with finite element (FE) results (a). Comparison with experiments (b).

Although the approach is a straightforward extension of that presented in section 2, the good agreement with finite element solutions indicates that the process of averaging over the stress orientations can provide good estimates of the biaxial compressive strength of SFRC. The semi-analytical estimate of biaxial compressive strength perfectly fit the experimental results of [3] that have used cubic specimen for their tests ($10 \times 10 \times 10 \text{ cm}^3$). The discrepancy observed as regards the comparison with those [5] can be explained in part by the size of specimen used by authors. Indeed,

these specimens (15x15x5 cm³) had higher dimensions parallel to the principal direction of biaxial solicitation, corresponding to higher concentration of fibers along the largest dimensions that are coincident with the loading directions.

4.2 Uniaxial compressive strength

The loading of the REV is now defined by an uniaxial compressive solicitation defined as $\underline{\underline{\Sigma}} = \Sigma \underline{e}_{III} \otimes \underline{e}_{III}$, with $\Sigma < 0$. The orientation of the unit vectors $\underline{e}_{III} = [\cos \varphi \sin \theta, \sin \varphi \sin \theta, \cos \theta]^T$ is defined by two angles (θ, φ) (spherical angles) with respect to the fixed frame $(\underline{e}_x, \underline{e}_y, \underline{e}_z)$ of fibers (Figure 4).

The first step consists in evaluating the strength under uniaxial compressive stress $\Sigma^-(\theta, \varphi)$. The minimization procedure defined in Eq. (5) applied to the considered solicitation leads to:

$$\Sigma^-(\theta, \varphi) = \min \left\{ \Sigma \mid \underline{\underline{\Sigma}} = \Sigma \underline{e}_{III} \otimes \underline{e}_{III} ; \underline{\underline{\sigma}}^m = \underline{\underline{\Sigma}} - \sum_{i=1}^3 \sigma_f \underline{e}_f \otimes \underline{e}_f ; \right. \\ \left. F^m(\underline{\underline{\sigma}}^m) \leq 0 ; |\sigma_f| \leq f_f \sigma_f^+, f = x, y, z \right\} \quad (21)$$

or, after mathematical developments

$$\Sigma^-(\theta, \varphi) = \min \left\{ \frac{\sum_{f=1}^3 \sigma_f (3(\underline{e}_{III} \cdot \underline{e}_f)^2 - 1 - 2\alpha_m^2) - 2\alpha_m (\alpha_m + 1) \sigma_m - \sqrt{\beta}}{2(1 - \alpha_m^2)}, |\sigma_f| \leq f_f \sigma_f^+, f = x, y, z \right\} \quad (22)$$

$$\beta = \left(-\sum_{f=1}^3 \sigma_f (3(\underline{e}_{III} \cdot \underline{e}_f)^2 - 1 - 2\alpha_m^2) + 2\alpha_m (\alpha_m + 1) \sigma_m \right)^2$$

$$- 4(1 - \alpha_m^2) \left(-\left(\sigma_m + \sum_{f=1}^3 \sigma_f \right) \alpha_m + \sigma_m \right)^2 + \sum_{f=1}^3 \sigma_f^2 - \sigma_x \sigma_y - \sigma_y \sigma_z - \sigma_z \sigma_x$$

Due to the complexity of an analytical determination of $\Sigma^-(\theta, \varphi)$, the latter is computed numerically as in the case of biaxial solicitation. The second step of the approach consists in adopting for the uniaxial compressive strength the average value

$$f_c = \langle \Sigma^- \rangle = \frac{1}{2\pi^2} \int_0^{2\pi} \int_0^\pi \Sigma^-(\varphi, \theta) d\theta d\varphi \quad (23)$$

Reconsidering the same data as in section 4.1, Figure 6(a) shows the variations of f_c versus the fiber volume fraction, together with the finite element results.

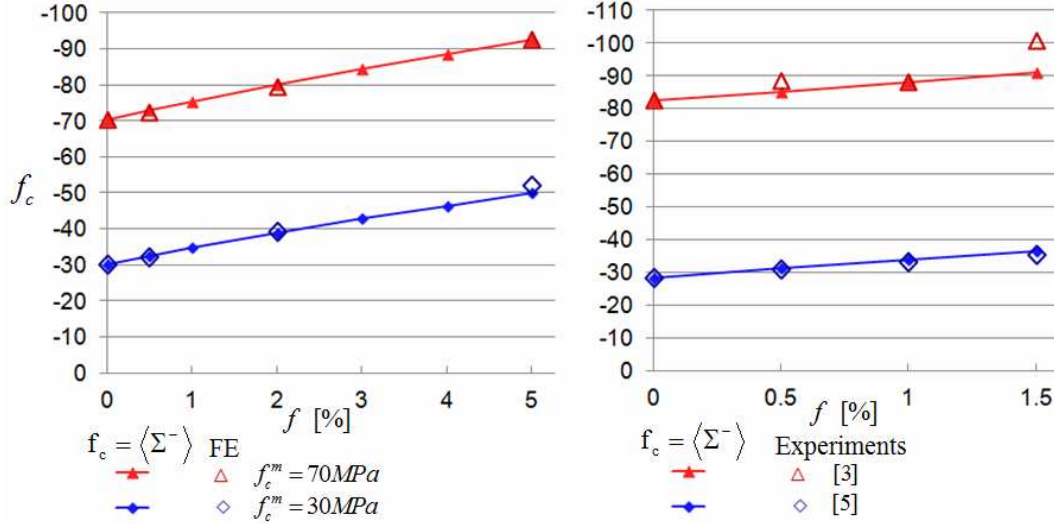


Figure 6. Comparison of uniaxial compressive strength estimates $f_c = \langle \Sigma^- (\underline{e}_{III}) \rangle$ (a) with FE analysis results and (b) with experimental results.

The results plotted in Figure 6(a) give evidence of the accuracy of the estimates based on averaging over the orientations of sollicitation. It is recalled that this averaging process is a simplified way to derive isotropic estimates for the homogenized strength properties.

The relevancy of the approach is also assessed by comparing the semi-analytical estimates with the experimental results given in [3] and [5], which have already been described in the previous section. These comparisons are shown in Figure 6(b), which emphasizes the relevancy of the semi-analytical approach.

Comments

The averaging approach has prove successful when applied to assessment of strength properties of SFRC under biaxial or uniaxial compressive stresses. The approach can obviously be extended to any stress orientation $\underline{\underline{\Sigma}} = \underline{\underline{\Sigma}}(\Sigma_I, \Sigma_{II}, \Sigma_{III}, \theta, \varphi, \psi)$. For a given stress orientation, the strength domain $\tilde{G}^{\text{hom}}(\theta, \varphi, \psi)$ is determined from minimization procedure (5). An isotropic approximation of the strength domain of SFRC is thus derived by averaging all stress states of $\tilde{G}^{\text{hom}}(\theta, \varphi, \psi)$, and then can be symbolically denoted by $G^{\text{hom}} = \langle \tilde{G}^{\text{hom}}(\theta, \varphi, \psi) \rangle$.

It is worth noting that the strength parameters adopted for the steel bars and the concrete matrix in the fictitious material are the real properties of the random medium. The comparison of the obtained analytical and numerical and experimental results indicates that for usual values of the aspect ratio l/d , the use of real properties for the characterization of the fictitious medium may be appropriate. Indeed previous experimental studies, as well as the present numerical analysis, seem to indicate that the aspect ratio has little influence on the uniaxial tensile and compressive strengths of FRC. Further numerical analyses involving a larger number of finite elements are needed to investigate the effect of l/d on the composite strength. Keeping in mind the small value of fiber content, such a task would be, however, to excessive in terms of computational cost. As a matter of fact, the practical values of f range between 0.5 and 5% and the influence of l/d within this range is not expected to be significant.

5 CONCLUSIONS

The strength properties of steel FRC were evaluated in this work through the homogenization and limit analysis theories. Assuming the existence of a correlation between the random medium (FRC) and a fictitious medium defined by a concrete matrix reinforced by long fibers, the strength domain of this material was obtained analytically. The composite strength criterion was determined considering the constituents (fibers and matrix) volume fractions and strength properties. In the fibers case, only its uniaxial compressive and tensile strengths are needed. The matrix concrete strength, in turn, was characterized by the Drucker Prager criterion. This criterion has a simpler formulation than the Ottosen and the Willam-Warnke criteria, for example, not allowing the characterization of the concrete behavior under tensile and compressive stress states with the same parameters. Nevertheless, it allows performing the proposed study, employing the homogenization and limit analysis theories, in an analytical way.

To address the relevancy as well as the accuracy of the analytical model, a finite element approach to the strength properties of FRC has been developed. It is based on the numerical resolution of the limit analysis problem formulated on the representative elementary volume of the random heterogeneous FRC.

It follows from the comparison of the two approaches that the analytical predictions derived from the fictitious medium formed by concrete matrix and long fibers oriented in three perpendicular directions overestimate the strength capacities of FRC when, in the analytical model, the principal directions of loading coincide with the fibers directions. In addition, the average of the analytical strength obtained for the fictitious medium considering all directions the fibers could take leads to results that satisfactorily fit the FE solutions and also experimental data of uniaxial and biaxial compressive strength. This good approximation indicates that the approach adopted for the uniaxial and biaxial compressive strengths calculation can provide good estimates of these properties.

Important extensions of the analysis to be foreseen in the future are to account for the fiber/matrix interface strength, to introduce a tensile cut-off in the formulation of the concrete matrix failure condition and to compare the analytical results with the few available experimental data. Moreover, the analysis of the FRC behavior employing a more complex model with a larger number of directions of fibers that would better considerate the isotropy of the material is a task which remains to be done.

REFERENCES

- [1] W.S. Yin, E.C.M. Su, M.A. Mansur, T.T.C. Hsu, 1989, "Biaxial tests of plain and fiber concrete", *ACI Mater. J.*, 86, 236–243.
- [2] L.A. Traina, S.A. Mansour, 1991, "Biaxial strength and deformational behavior of plain and steel fiber concrete", *ACI Mater. J.*, 88, 354–362.
- [3] D.H. Lim, E.G. Nawy, 2005, "Behaviour of plain and steel-fibre-reinforced high-strength concrete under uniaxial and biaxial compression", *Mag. Concr. Res.*, 57, 603–610.
- [4] S. Swaddiwudhipong, P.E.C. Seow, 2006, "Modelling of steel fiber-reinforced concrete under multi-axial loads", *Cem. Concr. Res.*, 36, 1354-1361.
- [5] M.V.N.N. Peres, 2006, *Aparatos de Baixo Custo para Ensaio Biaxiais em Concretos Reforçados com Fibras de Aço*, Master Thesis, Federal University of Rio Grande do Sul, Brazil, in portuguese.

- [6] K. Murugappan, P. Paramasivam, K.H. Tan, 1993, "Failure Envelope for Steel-Fiber Concrete under Biaxial Compression", *J. Mater. Civ. Eng.*, 5, 436-446.
- [7] X.D. Hu, R. Day, P. Dux, 2003, "Biaxial Failure Model for Fiber Reinforced Concrete", *J. Mater. Civ. Eng.*, 15, 609-615.
- [8] P.E.C. Seow, S. Swaddiwudhipong, 2005, "Failure Surface for Concrete under Multiaxial Load—a Unified Approach", *J. Mater. Civ. Eng.*, 17, 219-228.
- [9] P. Suquet, *Analyse limite et homogénéisation*, 1983, "Macroscopic yield strength of a strip reinforced material", *C. R. Acad. Sci. Paris Ser II* 296, 1355-1358.
- [10] P. De Buhan, 1986, *Approche fondamentale du calcul à la rupture des sols renforcés*, PhD Thesis, Université Paris VI, in french.
- [11] A. Kelly, W.R. Tyson, 1965, "Tensile properties of fibre-reinforced metals: copper/tungsten and copper/molybdenum", *J. Mech. Phys. Solids*, 13, 329-350.
- [12] P. De Buhan, A. Taliercio, 1991, "A homogenization approach to the yield strength of composite materials", *Eur. J. Mech. A Solids*, 10, 129-150.
- [13] A. Taliercio, M. Rovati, G. Sacchi-Landriani, 1991, "Formulation of a macroscopic strength criterion for tridirectional fiber composites", *Mechanics of Composites at Elevated and Cryogenic Temperatures*, S.N. Singhal, W.F. Jones, C.T. Herakovich (Eds.), ASME, New York, 71–180.
- [14] A. E. Elwi, T.M. Hrudey, 1989, "Finite element model for curved embedded reinforcement", *J. Eng. Mech. Div.*, 115, 740-754.
- [15] V.F. Pasa Dutra, S. Maghous, A. Campos Filho, A.R. Pacheco, 2010, "A micromechanical approach to elastic and viscoelastic properties of fiber reinforced concrete", *Cem. Concr. Res.* 40, 460-472.